



## Optimal power flow analysis with circulatory system-based optimization algorithm

Hüseyin Bakır \*<sup>1</sup> 

<sup>1</sup>Dogus University, Department of Electronics and Automation, Türkiye, hbakir@dogus.edu.tr

Cite this study: Bakır, H. (2024). Optimal power flow analysis with circulatory system-based optimization algorithm. Turkish Journal of Engineering, 8 (1), 92-106

### Keywords

Optimal power flow  
Metaheuristic algorithms  
Power system planning  
Optimization

### Research Article

DOI: 10.31127/tuje.1282429

Received:13.04.2023

Revised: 25.05.2023

Accepted:29.05.2023

Published:15.09.2023



### Abstract

Optimal power flow (OPF) is a challenging optimization problem with a large number of variables and constraints. To overcome the OPF issue, high-performance optimization algorithms are needed. In this direction, this paper has been centered on the optimization of the OPF with the circulatory system-based optimization (CSBO) algorithm. The performance of the algorithm was evaluated on the IEEE 57- and 118-bus power networks for the optimization of non-convex OPF objectives, i.e., fuel cost, power loss, voltage deviation, and enhancement of voltage stability. The solution quality of CSBO is compared with state-of-the-art metaheuristic algorithms such as Artificial Rabbits Optimization (ARO), African Vultures Optimization Algorithm (AVOA), and Chaos Game Optimization (CGO). Based on the OPF results, it is seen that the best fuel cost and voltage deviation results are calculated to be 41666.2344 \$/h and 0.5871 p.u with the CSBO algorithm for the IEEE 57-bus power system. The CSBO algorithm obtained the best objective function results for the IEEE 118-bus power network with a fuel cost of 134934.3140 \$/h and a power loss of 16.4688 MW. In conclusion, the present paper reports that the CSBO is a powerful and efficient metaheuristic algorithm to solve the OPF problem.

## 1. Introduction

In today's world, the energy crisis is undoubtedly one of the major problems. With the increasing standard of living, population, and industrialization, energy is needed more and more day by day. The problems that arise from energy increasing demand affect the economy, environment, and social life, that is, every stage of sustainable development in a negative way [1]. The optimal use of available energy resources plays a vital role in alleviating these problems.

The optimal power flow (OPF) is of great importance for the cost-effective and reliable operation of electrical networks [2]. OPF minimizes the selected optimization objective subject to a variety of equality and inequality constraints [3]. In order to achieve the optimal network configuration generally the settings of the independent variables such as the active power of generation units, tap setting of the transformers, the output of shunt VAR compensators, and terminal voltages at generator buses are optimized [4, 5].

OPF is a non-convex optimization problem with high computational complexity [4, 5]. Solving the OPF problem is a challenging task for power system

researchers [6]. To cope with this, it has been observed that various metaheuristic optimization algorithms have been successfully applied to the solution of the OPF problem. For instance, Houssein et al. [7] obtained the OPF solutions of the IEEE 30-bus power system using an enhanced equilibrium optimizer (EEO). In another study, Ramesh et al. [8] used an improved mayfly algorithm (IMA) to solve the OPF problem under different load conditions. Premkumar et al. [9] presented a comparative performance analysis of ESHADE, SHADE-SFS, and SHADE-SAP algorithms in solving the OPF problem. In the study, simulation studies were carried out on two power systems (IEEE 30- and IEEE 118-bus) to demonstrate the effectiveness of the algorithms. The findings revealed that ESHADE designed with the superiority of feasible solution (SFS) and self-adaptive penalty (SAP) methods gives more successful OPF results compared to the SHADE-SFS, and SHADE-SAP. Kaur and Narang [10] obtained OPF solutions for IEEE 30-, 57-, and 118-bus test systems using invasive weed optimization improved by the space transformation search method. Bakır et al. [11] used the fitness-distance balance-based stochastic fractal search (FDB-SFS) algorithm for solving OPF configured with renewable energy sources and

voltage source converters. Sonmez et al. [12] achieved OPF solutions for the IEEE 30-bus power network using improved artificial ecosystem optimization with a fitness-distance balance strategy. Abd El-Sattar et al. [13] used the powerful variant of the salp swarm algorithm to obtain the optimal operation configuration of three IEEE power networks. Jangir et al. [14] proposed the many-objective teaching-learning-based optimizer (MaOTLBO) to obtain the OPF solutions of the IEEE 30-bus power system. The authors evaluated the performance of the proposed algorithm with optimization of the power loss, voltage stability index, fuel cost, voltage deviation, and emission objectives. The results showed that MaOTLBO offers better OPF solutions compared to MOEA/D-DR and NSGA-III algorithms. Pandya et al. [15] formulated a multi-objective OPF problem in the presence of renewable power (wind, solar PV, small-hydro). The authors proposed the multi-objective equilibrium optimizer (MOEO) to solve the OPF problem incorporating renewable power. Considering the IEEE 30-bus power system results are together, it is seen that the proposed algorithm is more successful than the competitor optimizers in terms of the quality of Pareto-optimal solutions and their distribution. Premkumar et al. [16] developed the many-objective gradient-based optimizer (MaOGBO) to solve multi-objective OPF problems of IEEE 30-, 57- and 118-bus power systems. In the study, the authors considered fuel cost, voltage stability, emission, voltage deviation, and active-reactive power loss objectives. The results obtained from the OPF case studies showed that the proposed algorithm is an effective method for solving multi-objective OPF problems of large-scale power systems.

From the literature survey, it can be observed that power system researchers have investigated the efficiency of various metaheuristic algorithms in the solution of the OPF problem. Findings obtained from the literature works showed that OPF solution quality is directly related to the exploration and balanced search capabilities of optimizers. Accordingly, it can be said that high-performance optimization algorithms are required to obtain high-quality solutions to the OPF problem. In this regard, testing novel metaheuristic algorithms in the solution of the OPF problem will be beneficial. This topic deserves further investigation. With this point of view, this paper has centered on the solution to the OPF problem with circulatory system-based optimization (CSBO) [17]. In the study, fuel cost, real power loss, enhancement of voltage stability, and voltage deviation objectives are optimized. Simulation studies are performed on IEEE 57- and 118-bus power networks. The obtained OPF solutions from the CSBO algorithm were compared with up-to-date metaheuristic algorithms such as Artificial Rabbits Optimization (ARO) [18], African Vultures Optimization Algorithm (AVOA) [19], and Chaos Game Optimization (CGO) [20].

The main contributions of the study can be summarized as follows:

- Application of CSBO algorithm to the solution of single and multi-objective OPF problems for the first time.

- Comparative performance analysis of CSBO with state-of-the-art metaheuristic algorithms such as ARO, AVOA, and CGO.
- Optimization of fuel cost, power loss, voltage deviation, and voltage stability enhancement objectives on IEEE 57- and 118-bus power networks.
- Wilcoxon signed-rank test is applied to evaluate algorithm performance.

The remaining sections of the paper are structured as follows: Section 2 gives the definition of the OPF problem. In this direction, the dependent variables, independent variables, and constraints of the OPF problem are introduced. The optimization model of the CSBO algorithm is elaborated in Section 3. Section 4 summarizes and discusses the simulation results of the OPF case studies. Finally, conclusions of the study are presented in Section 5.

## 2. Formulation of OPF Problem

OPF is defined as the minimization of the selected objective function subject to various equality and inequality constraints. The optimization model of the OPF can be written as shown in Equation (1) [21, 22].

$$\begin{aligned} & \text{Minimize } O(s, c) \\ & \text{subject to } \begin{cases} g(s, c) = 0 \\ h(s, c) \leq 0 \end{cases} \end{aligned} \quad (1)$$

where  $O$  shows the objective function,  $s$  and  $c$  are the dependent and independent variable vectors of the OPF problem.  $g(s, c)$  and  $h(s, c)$  represent the set of equality and inequality constraints.

### 2.1. Dependent variables

The active power of the swing bus ( $P_{g_{swing}}$ ), the voltage value of the load bus ( $V_l$ ), the reactive power of the generator bus ( $Q_g$ ), and the transmission line loading ( $S_L$ ) are the dependent variables. Equation (2) gives the dependent variables vector ( $s$ ). In the equation,  $NPQ$ ,  $NG$ , and  $NL$  show the number of load buses, generator buses, and transmission lines.

$$s = [P_{g_{swing}}, V_{l_1} \dots V_{l_{NPQ}}, Q_{g_1} \dots Q_{g_{NG}}, S_{L_1} \dots S_{L_{NL}}] \quad (2)$$

### 2.2. Independent variables

Equation (3) gives the independent variables vector ( $c$ ) of the OPF problem

$$c = [P_{g_2} \dots P_{g_{NG}}, V_{g_1} \dots V_{g_{NG}}, Q_{c_1} \dots Q_{c_{NC}}, T_1 \dots T_{NT}] \quad (3)$$

where  $P_g$  is the active power of generation units except the swing generator,  $V_g$  represents the voltage magnitude of the generator buses.  $Q_c$  and  $T$  indicate the output of shunt VAR compensators and the tap setting of transformers, respectively.  $NT$  and  $NC$  represent the number of transformers and shunt VAR compensators.

### 2.3. OPF constraints

Active and reactive power balance Equations (4-5) are the equality constraints of the OPF problem [22].

#### 2.3.1. Equality constraints

$$P_{g_m} - P_{d_m} - V_m \sum_{n=1}^{NB} V_n [G_{mn} \cos(\delta_m - \delta_n) + B_{mn} \sin(\delta_m - \delta_n)] = 0 \quad \forall m \in NB \quad (4)$$

$$Q_{g_m} - Q_{d_m} - V_m \sum_{n=1}^{NB} V_n [G_{mn} \sin(\delta_m - \delta_n) + B_{mn} \cos(\delta_m - \delta_n)] = 0 \quad \forall m \in NB \quad (5)$$

where  $P_d$  and  $Q_d$  indicate active and reactive power demands.  $G_{mn}$  and  $B_{mn}$  are conductance and susceptance between bus  $m$  and bus  $n$ .  $NB$  shows the number of buses.

$$FC(P_g) = \sum_{i=1}^{NG} p_i + r_i P_{g,i} + w_i P_{g,i}^2 \quad (13)$$

#### 2.3.2. Inequality constraints

The following inequality constraints (Equations 6-12) are considered to ensure the secure operation of power systems.

- Generator constraints

$$P_{g,k}^{min} \leq P_{g,k} \leq P_{g,k}^{max} \quad \forall k \in NG \quad (6)$$

$$Q_{g,k}^{min} \leq Q_{g,k} \leq Q_{g,k}^{max} \quad \forall k \in NG \quad (7)$$

$$V_{g,k}^{min} \leq V_{g,k} \leq V_{g,k}^{max} \quad \forall k \in NG \quad (8)$$

- Shunt capacitor constraints

$$Q_{c,k}^{min} \leq Q_{c,k} \leq Q_{c,k}^{max} \quad \forall k \in NC \quad (9)$$

- Transformer constraints

$$T_k^{min} \leq T_k \leq T_k^{max} \quad \forall k \in NT \quad (10)$$

- Security constraints

$$V_{l,k}^{min} \leq V_{l,k} \leq V_{l,k}^{max} \quad \forall k \in NPQ \quad (11)$$

$$|S_{L,k}| \leq S_{L,k}^{max} \quad \forall k \in NL \quad (12)$$

### 2.4. Objective functions

In the study, single and multi-objective OPF objectives were optimized. Multi-objective OPF problems are converted into single-objective optimization by weighting the objective functions and solved in that way.

#### 2.4.1. Single-objective OPF objectives

- Fuel cost

Fuel cost minimization is widely used objective function in OPF problems. Mathematically, the fuel cost objective function can be written as follows [22]:

where  $P_{g,i}$  shows the active power of  $i$ -th generator in MW.  $p_i$ ,  $r_i$ , and  $w_i$  represent the cost coefficients of the same generator.

- Voltage deviation

Voltage deviation is one of the most important indicators that reflects the voltage quality of the network. The voltage deviation objective function is formulated as the cumulative deviation of all load buses from the nominal value (1 p.u) [22].

$$VD = \left( \sum_{m=1}^{NPQ} |V_{l_m} - 1| \right) \quad (14)$$

- Power loss

Real power loss is inevitable in power systems due to the inherent resistance of transmission lines. The real power loss objective function can be modeled as follows [22]:

$$P_{loss} = \sum_{p=1}^{NL} G_{p,ij} [V_i^2 + V_j^2 - 2 V_i V_j \cos(\delta_{ij})] \quad (15)$$

- Enhancement of voltage stability

The L-index value of the load buses is an important indicator of voltage stability. This index takes values between 0 and 1. If the value of the L-index is close to 0, the power system is stable, and when it is 1, voltage collapse occurs. The L-index value of the  $j$ -th bus ( $L_j$ ) is calculated using Equation 16 [22]:

$$L_j = \left| 1 - \sum_{i=1}^{NG} F_{ji} \frac{V_i}{V_j} \right| \quad j = 1, 2, \dots, NPQ \quad (16)$$

The objective function of system stability can be formulated using Equation 17 [22]:

$$L_{max} = \max(L_j) \quad \text{where } j = 1, 2, \dots, NPQ \quad (17)$$

### 2.4.2. Multi-objective OPF objectives

- Optimization of both fuel cost and voltage deviation

The objective function including simultaneous optimization of fuel cost and voltage deviation is given in Equation (18). In the equation, the value of the weight coefficient is set to  $\lambda_{VD}=100$  [22].

$$O(s, c) = \sum_{i=1}^{NG} (p_i + r_i P_{g,i} + w_i P_{g,i}^2) + (\lambda_{VD} \times VD) \quad (18)$$

$$O(s, c) = \sum_{i=1}^{NG} (p_i + r_i P_{g,i} + w_i P_{g,i}^2) + (\lambda_L \times L_{max}) \quad (19)$$

### 3. Circulatory System-based Optimization

Circulatory system-based optimization (CSBO) is a bio-inspired optimization algorithm with a high convergence performance developed by Ghasemi et al. in 2022 [17]. The optimizer is inspired by the function of the body's blood vessels and mimics the pulmonary and systematic circulation to perform the optimization task. Its simple structure, easy applicability, and lack of user-defined parameters are important advantages. The optimization steps of the CSBO algorithm are described in detail below.

- Initialization

An initial population of blood particles is generated as shown in Equation (20). In that equation,  $N$  and  $D$  show

$$X_i^{new} = X_i + K_{i1} \times p_i \times (X_i - X_1) + K_{23} \times p_i \times (X_3 - X_2) \quad (21)$$

$$K_{ij} = \frac{f(X_j) - f(X_i)}{|f(X_j) - f(X_i)| + \epsilon} = \begin{cases} 1 & f(X_i) \leq f(X_j) \\ -1 & f(X_i) > f(X_j) \\ 0 & f(X_i) = f(X_j) \end{cases} \quad (22)$$

where  $K_{ij}$  indicates the direction of movement of the blood mass.  $p_i$  determines the amount of displacement. It takes a value between 0 and 1.

- Blood mass flow in the pulmonary circulation

The CSBO algorithm ranks the blood population at each iteration and directs the population's weakest solution candidates to the pulmonary circulation system (Equation 23).

$$X_i^{new} = X_i + \left(\frac{randn}{iter}\right) \times randc(1, D), i = 1:Nr \quad (23)$$

where  $randn$  shows the random normal number.  $iter$  represents the current iteration number.  $randc$  represents Cauchy probability distribution function. In this phase,  $p_i$  is updated based on the number of the weakest population ( $Nr$ ) (Equation 24).

- Optimization of both fuel cost and enhancement of voltage stability

Equation (19) gives the objective function used in the simultaneous optimization of both fuel cost and enhancement of voltage stability. In that equation, the value of the weight coefficient is set to  $\lambda_L=100$  [22].

the numbers of population size and design parameters. The position of the blood particles in the search space ( $X_i = [x_{i1}, x_{i2}, \dots, x_{iD}]$ ) represents a possible solution to the optimization problem.

$$P = \begin{bmatrix} X_1 \\ \vdots \\ X_N \end{bmatrix} = \begin{bmatrix} x_{11} & \cdots & x_{1D} \\ \vdots & \ddots & \vdots \\ x_{N1} & \cdots & x_{ND} \end{bmatrix}_{N \times D} \quad (20)$$

- Movement of blood particles in veins

This step of the circulation cycle determines the new position of the  $i$ -th blood particle ( $X_i^{new}$ ) using the particle's current position and fitness value (Equation 21).

$$p_i = rand(1, D), i = 1:Nr \quad (24)$$

- Blood mass flow in the systematic circulation

The remainder of the blood particles in the population ( $Nl = N-Nr$ ) enters the pulmonary circulation (Equation 25).

$$X_{i,j}^{new} = X_{1,j} + p_i \times (X_{3,j} - X_{2,j}) \quad (25)$$

In the systematic circulation, the value of  $p_i$  is updated as shown in Equation 26:

$$p_i = \frac{f(X_i) - f_{worst}}{f_{best} - f_{worst}}, i = 1:Nl \quad (26)$$

The search process lifecycle steps (movement of blood particles in the veins, pulmonary circulation, and systematic circulations) of the CSBO algorithm continue

until the termination criterion is met. The pseudocode of the CSBO algorithm is given in Figure 1 [17].

```

1. Begin
2. Create a random initial blood population ( $P$ ) as shown in Equation (20)
3. Calculate  $p_i$  using Equations (24) and (26)
4. iter  $\leftarrow$  0
5. FEs  $\leftarrow$  N
6. while FEs  $\leq$  maxFEs do
7.   iter  $\leftarrow$  iter + 1
8.   Step 1: Movement of blood particle in the veins
9.   for  $i=1:N$  do
10.    Calculate  $K_{i1}$  and  $K_{23}$  using Equation (22)
11.    Create a new blood particle using Equation (21)
12.    Update the new position of  $i$ -th blood particle
13.    FEs = FEs + 1
14.   end for
15.   Step 2: Pulmonary Circulation
16.   for  $i=1:Nr$  do
17.     for  $j=1:D$  do
18.       if rand > 0.9
19.         Apply pulmonary circulation using Equation (23)
20.       else
21.          $X_{i,j}^{new} = X_{i,j}$ 
22.       end if
23.     end for
24.     FEs = FEs + 1
25.     Calculate  $p_i$  using Equation (24)
26.   end for
27.   Step 3: Systematic Circulation
28.   for  $i=1:Nl$  do
29.     Apply systematic circulation using Equation (25)
30.     Update the new position of  $i$ -th blood particle
31.     Calculate  $p_i$  using Equation (26)
32.     FEs = FEs + 1
33.   end for
34.   Update the best solution
35. end while
36. Display the best solution

```

**Figure 1.** Pseudocode of CSBO algorithm.

Figure 2 gives the steps followed to solve the OPF problem with CSBO and other competitive optimization algorithms.

#### 4. Results and Analysis

This section presents a comparative performance analysis of the CSBO and other well-known optimization algorithms (ARO, AVOA, and CGO) in solving the OPF problem. The performance of the algorithms is tested for optimization of non-convex OPF objectives i.e., fuel cost, voltage deviation ( $VD$ ), enhancement of voltage stability (L-index), and real power loss ( $P_{loss}$ ). OPF case studies performed on IEEE 57- and 118-bus power systems are summarized in Table 1.

Data for IEEE 57- and 118-bus power networks are taken from [17, 23]. All algorithms were coded in MATLAB R2016a [24] software and simulation studies were performed on PC with 11th Gen Intel (R) Core (TM)

i5-1135G7 @ 2.40 GHz /16 GB RAM/x64-based processor. MATPOWER 7.1 [23, 25] package program was used for OPF power flow calculations. For each OPF case study, the optimization algorithms were run 30 times. The algorithms were run using the settings given in their original article. The maximum number of fitness function evaluations (maxFEs) was used as the termination criterion of the metaheuristic search process. The maxFEs value for OPF case studies on IEEE 57- and 118-bus power networks are set to 42000 and 300000, respectively.

**Table 1.** Configuration of OPF case studies.

Case no	IEEE 57-bus system			IEEE 118-bus system	
	Fuel Cost	$VD$	L-index	Fuel Cost	$P_{loss}$
Case-1	●				
Case-2	●	●			
Case-3	●		●		
Case-4		●			
Case-5				●	
Case-6					●

#### 4.1. Simulation results of OPF case studies

- Case-1: Optimization of fuel cost

In this case, the fuel cost of the IEEE 57-bus power system is optimized. The results of the fuel cost objective function obtained by metaheuristic optimization algorithms are given in Table 2. As can be seen from the table, the fuel cost value is calculated to be 41666.2344 \$/h, 41668.8301 \$/h, 41676.0759 \$/h, and 41668.1817 \$/h by CSBO, ARO, AVOA, and CGO algorithms, respectively. Based on the numerical data, it is seen that the CSBO method offered the best fuel cost value. To put it more clearly, the CSBO algorithm yielded a profit of 9.8415 \$/h, 2.5957 \$/h, and 1.9473 \$/h in fuel cost compared to the results of the AVOA, ARO, and CGO methods.

- Case-2: Optimization of both fuel cost and voltage deviation

Case-2 handles the simultaneous minimization of the fuel cost and voltage deviation objectives on an IEEE 57-bus power system. In the present OPF case, objective functions are weighted and transformed into a single-objective optimization framework as shown in Equation (18). Considering the simulation results given in Table 2, it is seen that the CSBO algorithm reaches the best fitness value with 41774.4578, while AVOA gives the worst result with 41780.1955. The fuel cost and voltage deviation objective function values obtained with CSBO are 41697.22 \$/h and 0.7723 p.u, respectively.

- Case-3: Optimization of both fuel cost and enhancement of voltage stability

In Case 3, simultaneous optimization of the both fuel cost and enhancement of voltage stability (L-index) on an IEEE 57-bus power system is studied. In this OPF case,

objective functions are weighted and converted into a single-objective optimization as shown in Equation (19). As can be seen in Table 2, the fitness value of Case-3 is obtained to be 41693.9633, 41696.7465, 41701.7993, and 41695.6204 by CSBO, ARO, AVOA, and CGO algorithms, respectively. Accordingly, CSBO gave the best

result, followed by CGO. In addition, ARO and CGO algorithms have obtained competitive results. The fuel cost and L-index objective function values were calculated to be 41666.10 \$/h and 0.2785 for the CSBO algorithm.

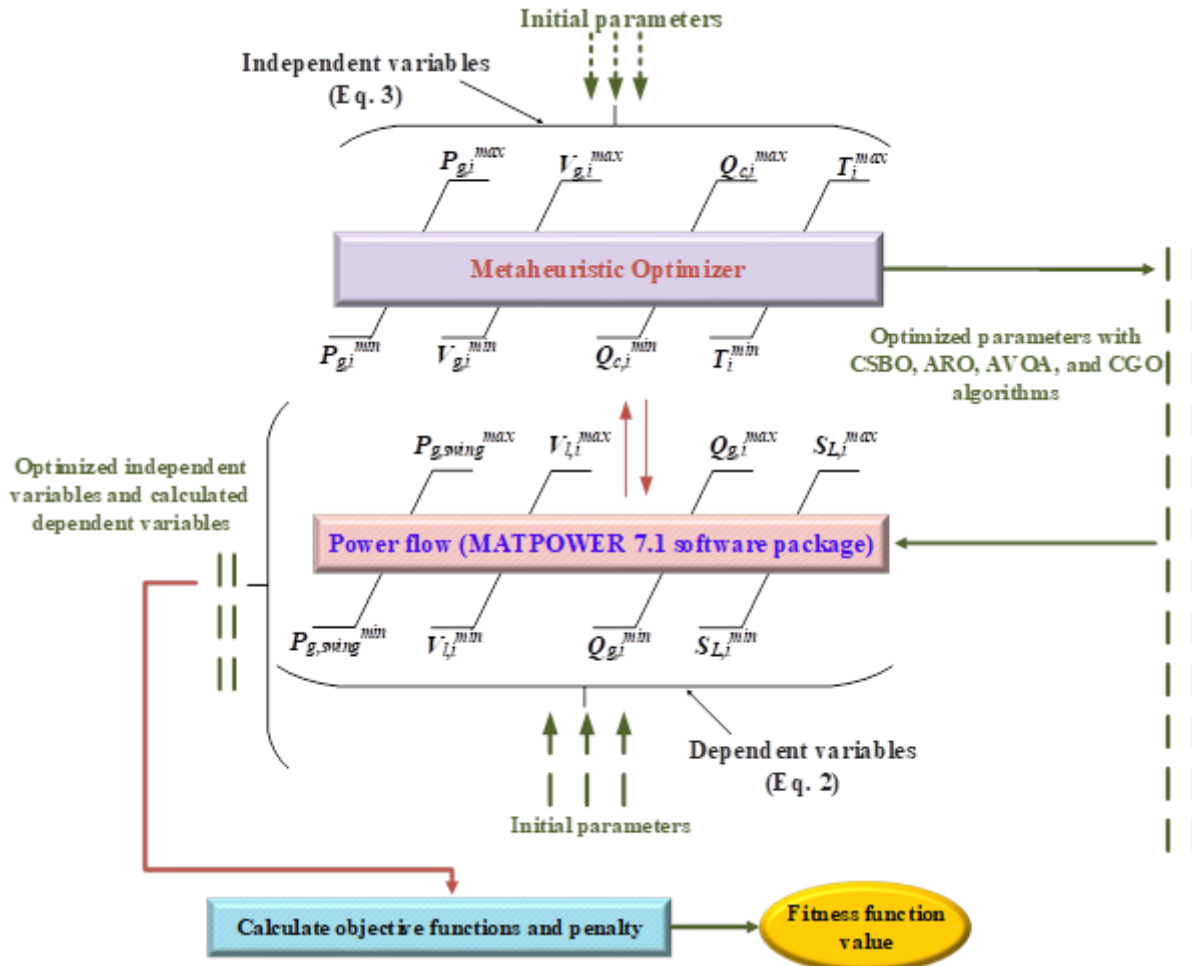


Figure 2. A flowchart for application of metaheuristic optimization algorithms to OPF problem.

- Case-4: Optimization of voltage deviation

Case-4 minimizes the voltage deviation of load buses in the IEEE 57-bus power network. As seen in Table 2, the voltage deviation value obtained by CSBO, ARO, AVOA, and CGO algorithms is 0.5871 p.u, 0.6151 p.u, 0.6329 p.u, and 0.6014 p.u, respectively. It is clear that the CSBO algorithm reached the best result, followed by CGO. In other words, CSBO reduced the voltage deviation by 4.5521%, 7.2365%, and 2.3777% compared to the ARO, AVOA, and CGO algorithms.

- Case-5: Optimization of fuel cost

This case aims to minimize the fuel cost of the IEEE 118-bus system. Based on the results given in Table 2, the fuel cost value is calculated to be 134934.3140 \$/h, 135023.4711 \$/h, 134985.7415 \$/h, and 135149.3384 \$/h for CSBO, ARO, AVOA, and CGO algorithms, respectively. From the numerical results, it is noticed that the CSBO method offered the best fuel cost value. To be more specific, the CSBO algorithm yielded a profit of

89.1571 \$/h, 51.4275 \$/h, and 215.0244 \$/h in fuel cost compared to the results of the ARO, AVOA, and CGO algorithms.

- Case-6: Optimization of active power loss

In Case-6, active power loss minimization of the IEEE 118-bus power system is performed. As can be seen from Table 2, the power loss objective function value is calculated to be 16.4688 MW, 17.3497 MW, 21.9025 MW, and 19.2740 MW by CSBO, ARO, AVOA, and CGO algorithms, respectively. Considering the numeric results, it is noticed that the CSBO offered the lowest active power loss value of 16.4688 MW. In other words, CSBO reduced the power loss by 5.0773%, 24.8085%, and 14.5543% compared to the ARO, AVOA, and CGO algorithms.

Given the results of OPF case studies are together, it is observed that the solution quality of the CSBO algorithm is superior compared to its competitors. The optimum parameter settings obtained with CSBO algorithm are given in Tables 3-5.

### 4.2. Convergence analysis

This subsection analyzes the convergence performance of metaheuristic algorithms for OPF case studies on IEEE 57- and 118-bus power systems. In this context, convergence curves were drawn to show the variation of the fitness value over the number of maxFES. Figure 3 gives the convergence curves of CSBO, ARO, AVOA, and CGO algorithms. Considering the convergence curves for the OPF case studies carried out on the IEEE 57-bus power system (Figure 3 a, b, c, d), it is seen that the CSBO and CGO algorithms exhibit a more successful search performance than their competitors. The convergence speed and solution quality of these two algorithms are impressive. On the other hand, it is seen that the ARO and AVOA algorithms cannot successfully converge to the global optimum. The underlying reason behind it is thought to be the premature convergence problem of these algorithms. From the convergence curves for the OPF case studies performed on the IEEE 118-bus power system (Figure 3 e, f), it is observed that the CSBO algorithm converges rapidly and produces better results than the compared ones.

### 4.3. Box-Plots

Box plots were prepared to observe the fitness value obtained by the algorithms over 30 independent runs. Each box plot includes the minimum, average, and maximum values of fitness value. A narrow box shows

that the algorithm exhibits a robust search performance. Figure 4 shows box plots of CSBO, ARO, AVOA, and CGO algorithms for OPF case studies. As is seen in the figure, the CSBO algorithm exhibited a stable and robust search performance in the optimization of OPF problems.

### 4.4. Statistical analysis

Performance metrics (minimum, mean, maximum, and standard deviation) calculated using data obtained from 30 runs are not sufficient to reveal the overall search performance of algorithms. In this context, statistical analysis of data is inevitable. This study applies Wilcoxon statistical test [35] for pairwise comparison between algorithms. Table 6 gives the Wilcoxon test results between CSBO and competitive algorithms. Considering ARO vs CSBO statistical test result for Case-1 (1/464), it is seen that ARO achieved a better fitness value than the CSBO algorithm for only run 1. In the remaining OPF cases, the fitness value of CSBO is better than ARO in all runs. Given the AVOA vs CSBO statistical test result, it is observed that the CSBO algorithm gave better OPF results compared to AVOA in all runs. Based on the CGO vs CSBO statistical test results for Case-3 and Case-4 (2/463), it is seen that CGO obtained a better fitness value than the CSBO algorithm for only run 2. In other OPF case studies, the CSBO algorithm is superior to CGO. In a nutshell, the Wilcoxon test results confirmed that the CSBO algorithm achieved better quality results than its competitors.

**Table 2.** Simulation results obtained from 30 runs.

Algorithm	Metric	Case-1	Case-2	Case-3	Case-4	Case-5	Case-6
CSBO	Best	<b>41666.2344</b>	<b>41774.4578</b>	<b>41693.9633</b>	<b>0.5871</b>	<b>134934.3140</b>	<b>16.4688</b>
	Mean	41667.3685	41774.9323	41694.9648	0.5925	134953.0728	16.9596
	Worst	41670.0940	41775.6829	41697.0897	0.6063	134984.2226	17.4696
	Std. Dev.	1.0878	0.3915	0.8563	0.0046	14.5031	0.2769
ARO	Best	41668.8301	41778.1130	41696.7465	0.6151	135023.4711	17.3497
	Mean	41673.4410	41784.0492	41701.5898	0.6524	135108.9051	18.7526
	Worst	41681.4971	41793.9520	41707.6488	0.7139	135260.7873	21.8958
	Std. Dev.	3.1497	4.8270	2.7930	0.0201	56.7417	0.9142
AVOA	Best	41676.0759	41780.1955	41701.7993	0.6329	134985.7415	21.9025
	Mean	41706.4203	41794.0997	41728.6458	0.7158	135143.2439	31.3293
	Worst	41764.5797	41813.8279	41782.6629	1.1610	135617.5325	45.3612
	Std. Dev.	22.5228	9.3521	19.2953	0.0936	156.7355	5.4363
CGO	Best	41668.1817	41775.6618	41695.6204	0.6014	135149.3384	19.2740
	Mean	41692.2616	41782.2631	41715.7907	0.6201	135253.7785	20.5832
	Worst	41771.7204	41825.9333	41759.5148	0.6798	135748.6388	23.3513
	Std. Dev.	23.5681	9.5836	19.8783	0.0193	106.5352	0.9733

### 4.5. Literature comparison

In this study, it has been observed that OPF solutions obtained with CSBO are of higher quality than ARO, AVOA, and CGO methods. However, the success of the CSBO algorithm against other literature studies is unknown. To clarify this state, the OPF solutions obtained by CSBO are compared with the available literature. The comparative results are given in Table 7. Given that all the results are together, it is noticed that the CSBO algorithm offered better-quality solutions than the literature studies.

### 5. Conclusion

This paper presents a comparative performance analysis of the metaheuristic algorithms in the optimization of single and multi-objective OPF problems. In this direction, CSBO, ARO, AVOA, and CGO algorithms are applied to obtain OPF solutions of IEEE 57- and 118-bus power systems. In the study, the fuel cost, voltage deviation, active power loss, and enhancement of voltage stability objectives are optimized. In the IEEE 57-bus power system, CSBO achieved 1.9473 \$/h and 2.3777% better results in terms of fuel cost and voltage deviation objectives compared to the CGO algorithm, which

exhibited the second-best performance. The CSBO algorithm reduced the fuel cost and power loss of the IEEE 118-bus power system by 51.4275 \$/h and 5.0773%, respectively. Considering the simulation results, it is seen that the CSBO algorithm obtained the best results for all OPF case studies under study. Convergence curves, box plots, and Wilcoxon statistical

test results showed that the CSBO algorithm exhibited a better convergence success compared to other optimizers considered in the study. The obtained OPF solutions from CSBO are compared with the literature studies and it is observed that the proposed algorithm gives better solutions.

**Table 3.** Optimum solutions of CSBO algorithm for IEEE 57-bus OPF case studies.

Parameters	Min	Max	Case-1	Case-2	Case-3	Case-4
$P_{G_{g_1}}$ (MW)	0	576	142.7350	142.6349	142.8443	352.9668
$P_{g_2}$ (MW)	30	100	89.2764	88.3179	89.3849	32.3379
$P_{g_3}$ (MW)	40	140	45.0011	45.0339	44.9871	134.2231
$P_{g_6}$ (MW)	30	100	70.7775	71.6483	70.8617	30.5596
$P_{g_8}$ (MW)	100	550	460.6593	460.3545	460.4950	272.6486
$P_{g_9}$ (MW)	30	100	96.9825	97.8728	96.8019	99.8451
$P_{g_{12}}$ (MW)	100	410	360.2274	360.5228	360.2750	348.9024
$Q_{g_1}$ (MVar)	-140	200	43.1142	40.8621	44.7284	-40.4167
$Q_{g_2}$ (MVar)	-17	50	49.9947	49.9932	49.9931	49.6062
$Q_{g_3}$ (MVar)	-10	60	30.9278	34.8576	35.6592	59.9374
$Q_{g_6}$ (MVar)	-8	25	-7.8592	-3.9786	-7.6921	-7.9544
$Q_{g_8}$ (MVar)	-140	200	53.6284	72.5680	49.7739	43.9786
$Q_{g_9}$ (MVar)	-3	9	8.9982	8.9983	8.9993	8.9826
$Q_{g_{12}}$ (MVar)	-150	155	60.1086	45.6496	58.3601	154.9041
$V_1$ (p.u)	0.95	1.10	1.0635	1.0333	1.0670	1.0081
$V_2$ (p.u)	0.95	1.10	1.0611	1.0317	1.0647	1.0064
$V_3$ (p.u)	0.95	1.10	1.0534	1.0272	1.0573	1.0165
$V_6$ (p.u)	0.95	1.10	1.0589	1.0427	1.0602	1.0019
$V_8$ (p.u)	0.95	1.10	1.0757	1.0627	1.0753	1.0214
$V_9$ (p.u)	0.95	1.10	1.0500	1.0285	1.0507	1.0107
$V_{12}$ (p.u)	0.95	1.10	1.0511	1.0191	1.0525	1.0392
$Q_{c18}$ (MVar)	0	20	7.9183	5.4348	8.4539	0.0436
$Q_{c25}$ (MVar)	0	20	13.7033	16.0706	13.1343	18.8307
$Q_{c53}$ (MVar)	0	20	12.3686	15.5759	12.0256	19.9985
$T_{19}$ (p.u)	0.90	1.10	0.9518	1.0443	0.9293	1.0425
$T_{20}$ (p.u)	0.90	1.10	1.0112	0.9529	1.0396	0.9447
$T_{31}$ (p.u)	0.90	1.10	1.0086	0.9902	1.0096	0.9691
$T_{35}$ (p.u)	0.90	1.10	1.0535	0.9325	1.0469	1.0986
$T_{36}$ (p.u)	0.90	1.10	0.9801	1.0999	0.9768	1.0190
$T_{37}$ (p.u)	0.90	1.10	1.0327	1.0219	1.0314	1.0022
$T_{41}$ (p.u)	0.90	1.10	0.9955	1.0181	0.9952	0.9948
$T_{46}$ (p.u)	0.90	1.10	0.9609	0.9390	0.9599	0.9195
$T_{54}$ (p.u)	0.90	1.10	0.9128	0.9000	0.9128	0.9000
$T_{58}$ (p.u)	0.90	1.10	0.9790	0.9671	0.9817	0.9310
$T_{59}$ (p.u)	0.90	1.10	0.9639	0.9648	0.9673	0.9831
$T_{65}$ (p.u)	0.90	1.10	0.9753	0.9850	0.9763	1.0184
$T_{66}$ (p.u)	0.90	1.10	0.9388	0.9369	0.9398	0.9000
$T_{71}$ (p.u)	0.90	1.10	0.9738	0.9699	0.9743	0.9631
$T_{73}$ (p.u)	0.90	1.10	0.9919	0.9983	0.9924	1.0017
$T_{76}$ (p.u)	0.90	1.10	0.9627	0.9425	0.9689	0.9087
$T_{80}$ (p.u)	0.90	1.10	1.0004	1.0078	1.0041	0.9920
Fuel Cost (\$/h)	-	-	<b>41666.2344</b>	<b>41697.22</b>	<b>41666.10</b>	48524.40
$P_{loss}$ (MW)	-	-	14.8593	15.5851	14.8500	20.3134
$VD$ (p.u)	-	-	1.7033	<b>0.7723</b>	1.7059	<b>0.5871</b>
L-index	-	-	0.2789	0.2930	<b>0.2785</b>	0.3008

**Table 4.** Optimum solutions of CSBO algorithm for Case-5.

Parameters	Bounds	Values	Parameters	Values	Parameters	Values
$P_{g_1}$ (MW)	30-100	30.0000	$V_{g_1}$ (p.u)	1.0341	$Q_{c5}$ (MVar)	24.9998
$P_{g_4}$ (MW)	30-100	30.0002	$V_g$ (p.u)	1.0594	$Q_{c34}$ (MVar)	0.1247
$P_{g_6}$ (MW)	30-100	30.0000	$V_{g_6}$ (p.u)	1.0531	$Q_{c37}$ (MVar)	0.0017
$P_{g_8}$ (MW)	30-100	30.0001	$V_{g_8}$ (p.u)	1.0404	$Q_{c44}$ (MVar)	3.5609
$P_{g_{10}}$ (MW)	165-550	315.8477	$V_{g_{10}}$ (p.u)	1.0483	$Q_{c45}$ (MVar)	18.8540
$P_{g_{12}}$ (MW)	55.5-185	67.3771	$V_{g_{12}}$ (p.u)	1.0489	$Q_{c46}$ (MVar)	0.0002
$P_{g_{15}}$ (MW)	30-100	30.0000	$V_{g_{15}}$ (p.u)	1.0455	$Q_{c48}$ (MVar)	7.0132
$P_{g_{18}}$ (MW)	30-100	30.0000	$V_{g_{18}}$ (p.u)	1.0474	$Q_{c74}$ (MVar)	24.9925
$P_{g_{19}}$ (MW)	30-100	30.0000	$V_{g_{19}}$ (p.u)	1.0455	$Q_{c79}$ (MVar)	24.9999
$P_{g_{24}}$ (MW)	30-100	30.0002	$V_{g_{24}}$ (p.u)	1.0587	$Q_{c82}$ (MVar)	24.9442
$P_{g_{25}}$ (MW)	96-320	152.2763	$V_{g_{25}}$ (p.u)	1.0718	$Q_{c83}$ (MVar)	13.0013
$P_{g_{26}}$ (MW)	124.2-414	220.4765	$V_{g_{26}}$ (p.u)	1.08288	$Q_{c105}$ (MVar)	24.8915
$P_{g_{27}}$ (MW)	30-100	30.0000	$V_{g_{27}}$ (p.u)	1.0506	$Q_{c107}$ (MVar)	24.8057
$P_{g_{31}}$ (MW)	32.1-107	32.1000	$V_{g_{31}}$ (p.u)	1.0465	$Q_{c110}$ (MVar)	24.9997
$P_{g_{32}}$ (MW)	30-100	30.0000	$V_{g_{32}}$ (p.u)	1.0489	$T_8$ (p.u)	0.9857
$P_{g_{34}}$ (MW)	30-100	30.0000	$V_{g_{34}}$ (p.u)	1.0496	$T_{32}$ (p.u)	1.0644
$P_{g_{36}}$ (MW)	30-100	30.0000	$V_{g_{36}}$ (p.u)	1.0474	$T_{36}$ (p.u)	0.9804
$P_{g_{40}}$ (MW)	30-100	30.00000	$V_{g_{40}}$ (p.u)	1.0339	$T_{51}$ (p.u)	0.9858
$P_{g_{42}}$ (MW)	30-100	30.0006	$V_{g_{42}}$ (p.u)	1.0360	$T_{93}$ (p.u)	0.9810
$P_{g_{46}}$ (MW)	35.7-119	35.7000	$V_{g_{46}}$ (p.u)	1.0524	$T_{95}$ (p.u)	1.0013
$P_{g_{49}}$ (MW)	91.2-304	161.7616	$V_{g_{49}}$ (p.u)	1.0618	$T_{102}$ (p.u)	0.9653
$P_{g_{54}}$ (MW)	44.4-148	44.4039	$V_{g_{54}}$ (p.u)	1.0418	$T_{107}$ (p.u)	0.9431
$P_{g_{55}}$ (MW)	30-100	30.0000	$V_{g_{55}}$ (p.u)	1.0415	$T_{127}$ (p.u)	0.9895
$P_{g_{56}}$ (MW)	30-100	30.0007	$V_{g_{56}}$ (p.u)	1.0414	Fuel Cost (\$/h)	<b>134934.3140</b>
$P_{g_{59}}$ (MW)	76.5-255	124.7872	$V_{g_{59}}$ (p.u)	1.0598	$VD$ (p.u)	2.9658
$P_{g_{61}}$ (MW)	78-260	122.7446	$V_{g_{61}}$ (p.u)	1.0616	$P_{loss}$ (MW)	57.8922
$P_{g_{62}}$ (MW)	30-100	30.0000	$V_{g_{62}}$ (p.u)	1.0569	$P_{G_{69}}$ (Swing Bus)	370.0572
$P_{g_{65}}$ (MW)	147.3-491	289.0389	$V_{g_{65}}$ (p.u)	1.0622		
$P_{g_{66}}$ (MW)	147.6-492	288.9684	$V_{g_{66}}$ (p.u)	1.0731		
$P_{g_{70}}$ (MW)	30-100	30.0004	$V_{g_{69}}$ (p.u)	1.0701		
$P_{g_{72}}$ (MW)	30-100	30.0000	$V_{g_{70}}$ (p.u)	1.0554		
$P_{g_{73}}$ (MW)	30-100	30.0001	$V_{g_{72}}$ (p.u)	1.0625		
$P_{g_{74}}$ (MW)	30-100	30.0008	$V_{g_{73}}$ (p.u)	1.0597		
$P_{g_{76}}$ (MW)	30-100	30.0001	$V_{g_{74}}$ (p.u)	1.0420		
$P_{g_{77}}$ (MW)	30-100	30.0000	$V_{g_{76}}$ (p.u)	1.0233		
$P_{g_{80}}$ (MW)	173.1-577	348.5164	$V_{g_{77}}$ (p.u)	1.0480		
$P_{g_{85}}$ (MW)	30-100	30.0003	$V_{g_{80}}$ (p.u)	1.0562		
$P_{g_{87}}$ (MW)	31.2-104	31.2000	$V_{g_{85}}$ (p.u)	1.0600		
$P_{g_{89}}$ (MW)	212.1-707	384.3456	$V_{g_{87}}$ (p.u)	1.0759		
$P_{g_{90}}$ (MW)	30-100	30.0000	$V_{g_{89}}$ (p.u)	1.0723		
$P_{g_{91}}$ (MW)	30-100	30.0000	$V_{g_{90}}$ (p.u)	1.0573		
$P_{g_{92}}$ (MW)	30-100	30.0002	$V_{g_{91}}$ (p.u)	1.0622		
$P_{g_{99}}$ (MW)	30-100	30.0000	$V_{g_{92}}$ (p.u)	1.0612		
$P_{g_{100}}$ (MW)	105.6-352	177.4768	$V_{g_{99}}$ (p.u)	1.0582		
$P_{g_{103}}$ (MW)	42-140	42.0007	$V_{g_{100}}$ (p.u)	1.0605		
$P_{g_{104}}$ (MW)	30-100	30.0001	$V_{g_{103}}$ (p.u)	1.0578		
$P_{g_{105}}$ (MW)	30-100	30.0002	$V_{g_{104}}$ (p.u)	1.0531		
$P_{g_{107}}$ (MW)	30-100	30.0000	$V_{g_{105}}$ (p.u)	1.0507		
$P_{g_{110}}$ (MW)	30-100	30.0000	$V_{g_{107}}$ (p.u)	1.0441		
$P_{g_{111}}$ (MW)	40.8-136	40.8000	$V_{g_{110}}$ (p.u)	1.0529		
$P_{g_{112}}$ (MW)	30-100	30.0000	$V_{g_{111}}$ (p.u)	1.0619		
$P_{g_{113}}$ (MW)	30-100	30.0000	$V_{g_{112}}$ (p.u)	1.0442		
$P_{g_{116}}$ (MW)	30-100	30.0001	$V_{g_{113}}$ (p.u)	1.0555		
			$V_{g_{116}}$ (p.u)	1.0600		

**Table 5.** Optimum solutions of CSBO algorithm for Case-6.

Parameters	Bounds	Values	Parameters	Values	Parameters	Values
$P_{g_1}$ (MW)	30-100	69.6586	$V_{g_1}$ (p.u)	1.0418	$Q_{c5}$ (MVar)	18.8284
$P_{g_4}$ (MW)	30-100	30.0001	$V_g$ (p.u)	1.0566	$Q_{c34}$ (MVar)	0.0007
$P_{g_6}$ (MW)	30-100	30.3765	$V_{g_6}$ (p.u)	1.0527	$Q_{c37}$ (MVar)	0.0006
$P_{g_8}$ (MW)	30-100	30.0081	$V_{g_8}$ (p.u)	1.0375	$Q_{c44}$ (MVar)	4.6913
$P_{g_{10}}$ (MW)	165-550	165.0001	$V_{g_{10}}$ (p.u)	1.0451	$Q_{c45}$ (MVar)	17.7797
$P_{g_{12}}$ (MW)	55.5-185	134.5671	$V_{g_{12}}$ (p.u)	1.0514	$Q_{c46}$ (MVar)	24.9838
$P_{g_{15}}$ (MW)	30-100	87.3883	$V_{g_{15}}$ (p.u)	1.0502	$Q_{c48}$ (MVar)	7.47022
$P_{g_{18}}$ (MW)	30-100	30.0006	$V_{g_{18}}$ (p.u)	1.0501	$Q_{c74}$ (MVar)	24.9999
$P_{g_{19}}$ (MW)	30-100	60.1661	$V_{g_{19}}$ (p.u)	1.0496	$Q_{c79}$ (MVar)	24.9971
$P_{g_{24}}$ (MW)	30-100	30.0002	$V_{g_{24}}$ (p.u)	1.0579	$Q_{c82}$ (MVar)	24.9465
$P_{g_{25}}$ (MW)	96-320	96.0000	$V_{g_{25}}$ (p.u)	1.0671	$Q_{c83}$ (MVar)	10.9260
$P_{g_{26}}$ (MW)	124.2-414	124.2000	$V_{g_{26}}$ (p.u)	1.0546	$Q_{c105}$ (MVar)	24.9992
$P_{g_{27}}$ (MW)	30-100	48.4661	$V_{g_{27}}$ (p.u)	1.0525	$Q_{c107}$ (MVar)	0.15651
$P_{g_{31}}$ (MW)	32.1-107	62.2590	$V_{g_{31}}$ (p.u)	1.0519	$Q_{c110}$ (MVar)	18.5319
$P_{g_{32}}$ (MW)	30-100	37.1864	$V_{g_{32}}$ (p.u)	1.0518	$T_8$ (p.u)	0.98264
$P_{g_{34}}$ (MW)	30-100	65.6885	$V_{g_{34}}$ (p.u)	1.0462	$T_{32}$ (p.u)	1.04261
$P_{g_{36}}$ (MW)	30-100	55.2984	$V_{g_{36}}$ (p.u)	1.0435	$T_{36}$ (p.u)	0.97987
$P_{g_{40}}$ (MW)	30-100	99.9999	$V_{g_{40}}$ (p.u)	1.0403	$T_{51}$ (p.u)	0.98036
$P_{g_{42}}$ (MW)	30-100	99.9987	$V_{g_{42}}$ (p.u)	1.0387	$T_{93}$ (p.u)	1.00009
$P_{g_{46}}$ (MW)	35.7-119	81.1353	$V_{g_{46}}$ (p.u)	1.0364	$T_{95}$ (p.u)	0.99712
$P_{g_{49}}$ (MW)	91.2-304	142.2017	$V_{g_{49}}$ (p.u)	1.0349	$T_{102}$ (p.u)	0.97309
$P_{g_{54}}$ (MW)	44.4-148	147.9995	$V_{g_{54}}$ (p.u)	1.0294	$T_{107}$ (p.u)	0.96532
$P_{g_{55}}$ (MW)	30-100	70.3444	$V_{g_{55}}$ (p.u)	1.0289	$T_{127}$ (p.u)	0.96915
$P_{g_{56}}$ (MW)	30-100	99.9989	$V_{g_{56}}$ (p.u)	1.0288	Fuel Cost (\$/h)	155741.09
$P_{g_{59}}$ (MW)	76.5-255	254.1118	$V_{g_{59}}$ (p.u)	1.0282	$VD$ (p.u)	2.5323
$P_{g_{61}}$ (MW)	78-260	78.0000	$V_{g_{61}}$ (p.u)	1.0289	$P_{loss}$ (MW)	<b>16.4688</b>
$P_{g_{62}}$ (MW)	30-100	64.0547	$V_{g_{62}}$ (p.u)	1.0276	$P_{G_{69}}$ (Swing Bus)	3.4037
$P_{g_{65}}$ (MW)	147.3-491	147.3110	$V_{g_{65}}$ (p.u)	1.0349		
$P_{g_{66}}$ (MW)	147.6-492	147.6050	$V_{g_{66}}$ (p.u)	1.0362		
$P_{g_{70}}$ (MW)	30-100	30.0007	$V_{g_{69}}$ (p.u)	1.0419		
$P_{g_{72}}$ (MW)	30-100	30.0001	$V_{g_{70}}$ (p.u)	1.0439		
$P_{g_{73}}$ (MW)	30-100	30.0012	$V_{g_{72}}$ (p.u)	1.0567		
$P_{g_{74}}$ (MW)	30-100	96.1758	$V_{g_{73}}$ (p.u)	1.0499		
$P_{g_{76}}$ (MW)	30-100	99.9328	$V_{g_{74}}$ (p.u)	1.0413		
$P_{g_{77}}$ (MW)	30-100	99.9809	$V_{g_{76}}$ (p.u)	1.0314		
$P_{g_{80}}$ (MW)	173.1-577	286.763	$V_{g_{77}}$ (p.u)	1.0429		
$P_{g_{85}}$ (MW)	30-100	32.2496	$V_{g_{80}}$ (p.u)	1.0488		
$P_{g_{87}}$ (MW)	31.2-104	31.2013	$V_{g_{85}}$ (p.u)	1.0554		
$P_{g_{89}}$ (MW)	212.1-707	212.1151	$V_{g_{87}}$ (p.u)	1.0733		
$P_{g_{90}}$ (MW)	30-100	99.9387	$V_{g_{89}}$ (p.u)	1.0645		
$P_{g_{91}}$ (MW)	30-100	30.0060	$V_{g_{90}}$ (p.u)	1.0569		
$P_{g_{92}}$ (MW)	30-100	30.0003	$V_{g_{91}}$ (p.u)	1.0593		
$P_{g_{99}}$ (MW)	30-100	39.7779	$V_{g_{92}}$ (p.u)	1.0543		
$P_{g_{100}}$ (MW)	105.6-352	105.6001	$V_{g_{99}}$ (p.u)	1.0508		
$P_{g_{103}}$ (MW)	42-140	42.0015	$V_{g_{100}}$ (p.u)	1.0519		
$P_{g_{104}}$ (MW)	30-100	32.9776	$V_{g_{103}}$ (p.u)	1.0531		
$P_{g_{105}}$ (MW)	30-100	52.5637	$V_{g_{104}}$ (p.u)	1.0507		
$P_{g_{107}}$ (MW)	30-100	57.7776	$V_{g_{105}}$ (p.u)	1.0504		
$P_{g_{110}}$ (MW)	30-100	30.01218	$V_{g_{107}}$ (p.u)	1.0506		
$P_{g_{111}}$ (MW)	40.8-136	40.80305	$V_{g_{110}}$ (p.u)	1.0538		
$P_{g_{112}}$ (MW)	30-100	51.60743	$V_{g_{111}}$ (p.u)	1.0628		
$P_{g_{113}}$ (MW)	30-100	30.00222	$V_{g_{112}}$ (p.u)	1.0502		
$P_{g_{116}}$ (MW)	30-100	74.5478	$V_{g_{113}}$ (p.u)	1.0563		
			$V_{g_{116}}$ (p.u)	1.0326		

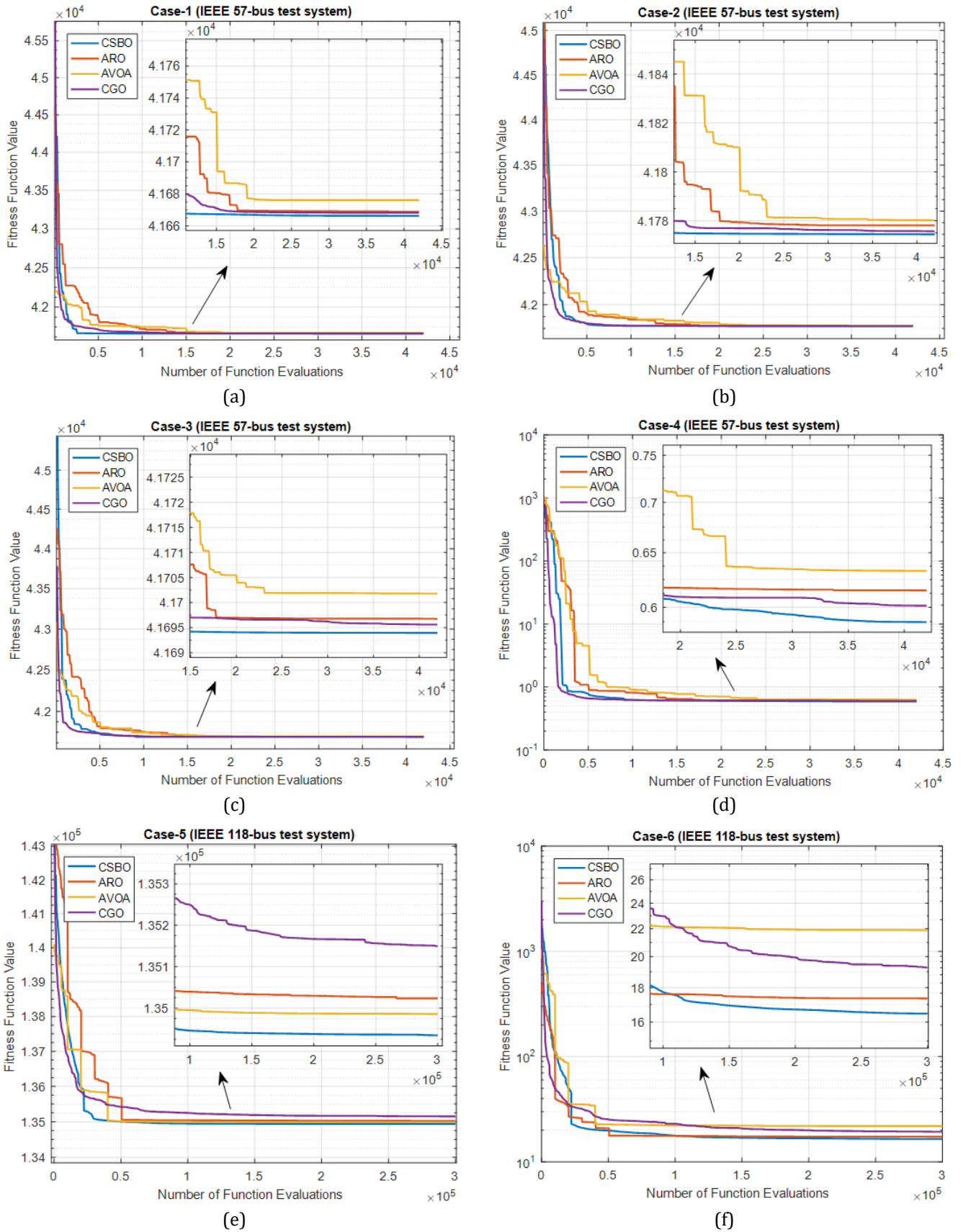
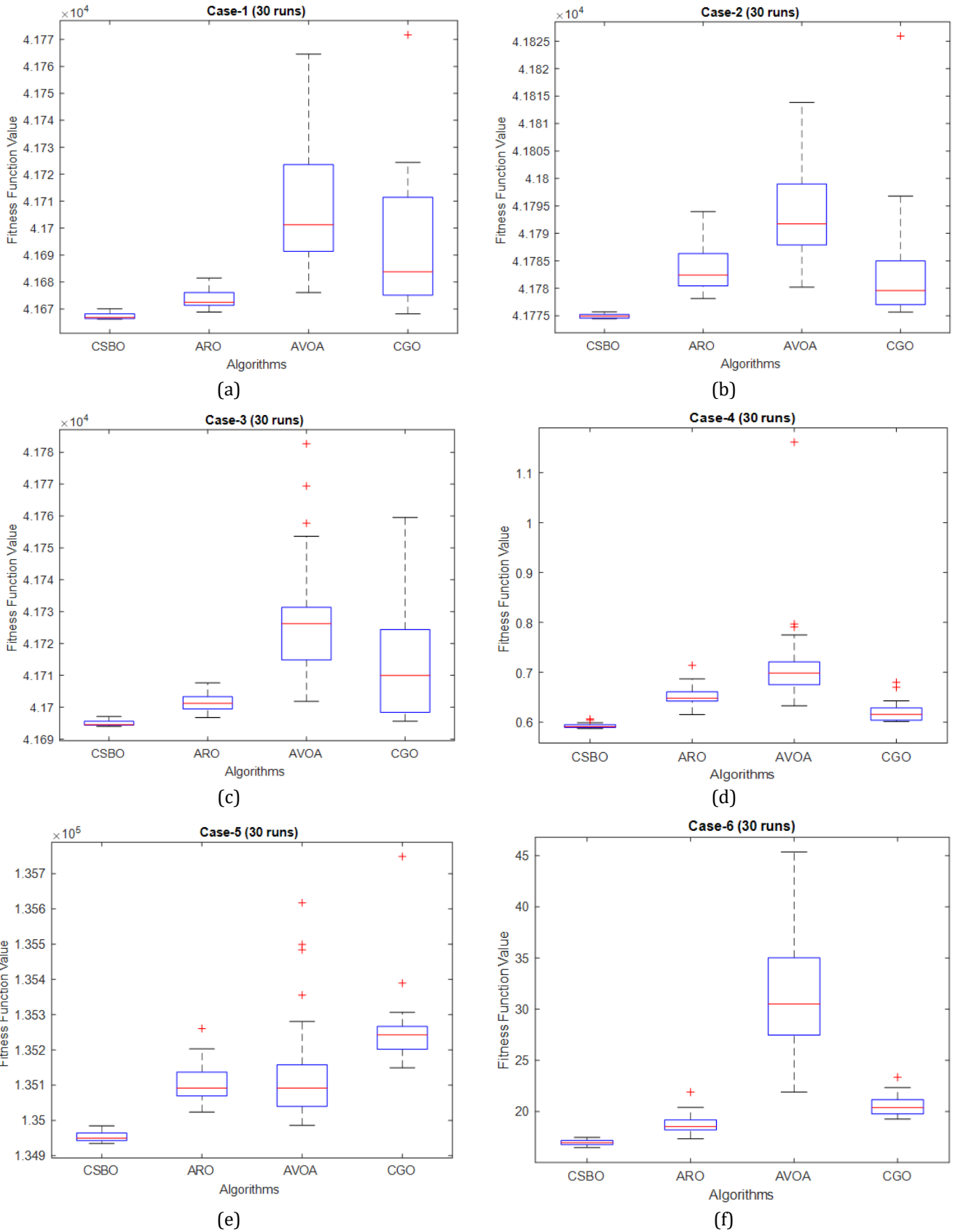


Figure 3. Convergence curves: (a) Case-1, (b) Case-2, (c) Case-3, (d) Case-4, (e) Case-5, (f) Case-6.



**Figure 4.** Box-plots for (a) Case-1, (b) Case-2, (c) Case-3, (d) Case-4, (e) Case-5 (f) Case-6.

**Table 6.** Wilcoxon test results.

Problem Cases	ARO vs CSBO			AVOA vs CSBO			CGO vs CSBO		
	R+	R-	p-value	R+	R-	p-value	R+	R-	p-value
Case-1	1	464	1.92 x 10 <sup>-6</sup>	0	465	1.73 x 10 <sup>-6</sup>	0	465	1.73 x 10 <sup>-6</sup>
Case-2	0	465	1.73 x 10 <sup>-6</sup>	0	465	1.73 x 10 <sup>-6</sup>	0	465	1.73 x 10 <sup>-6</sup>
Case-3	0	465	1.73 x 10 <sup>-6</sup>	0	465	1.73 x 10 <sup>-6</sup>	2	463	2.12 x 10 <sup>-6</sup>
Case-4	0	465	1.73 x 10 <sup>-6</sup>	0	465	1.73 x 10 <sup>-6</sup>	2	463	2.12 x 10 <sup>-6</sup>
Case-5	0	465	1.73 x 10 <sup>-6</sup>	0	465	1.73 x 10 <sup>-6</sup>	0	465	1.73 x 10 <sup>-6</sup>
Case-6	0	465	1.73 x 10 <sup>-6</sup>	0	465	1.73 x 10 <sup>-6</sup>	0	465	1.73 x 10 <sup>-6</sup>

**Table 7.** Comparison of the CSBO algorithm with literature studies.

Case no.	Algorithms	Best Fitness	Fuel Cost	$P_{loss}$	VD	L-index
Case-1	CSBO	<b>41666.23</b>	41666.23	14.8593	1.70336	0.2789
	SP-DE [22]	41667.82	41667.82	14.9090	1.54367	0.28123
	ECHT-DE [22]	41670.56	41670.56	14.9479	1.50319	0.28886
	SF-DE [22]	41667.85	41667.85	14.8864	1.64209	0.27971
	DE [26]	41682	41682	NA	NA	NA
	MSA [27]	41673.72	41673.72	15.0526	1.5508	0.28392
	ICBO [28]	41697.33	41697.33	15.5470	1.3173	0.27760
	DSA [29]	41686.82	41686.82	NA	1.0833	0.24353
	APFPA [30]	41628.75 <sup>a</sup>	41628.75 <sup>a</sup>	14.0470	3.5571 <sup>a</sup>	NA
	MICA-TLA [31]	41675.05	41675.05	15.0149	1.6161	NA
	ARCBBO [32]	41686	41686	15.3769	NA	NA
LTLBO [33]	41679.55	41679.55	15.1589	NA	NA	
Case-2	CSBO	<b>41774.45</b>	41697.22	15.5851	0.7723	0.2930
	SP-DE [22]	41774.75	41697.50	15.5897	0.7725	0.29228
	ECHT-DE [22]	41776.48	41694.82	15.5806	0.81659	0.29198
	SF-DE [22]	41775.09	41697.52	15.5616	0.77572	0.29262
	MSA [27]	41782.80	41714.98	15.9214	0.6782	0.29533
	MFO [27]	41786.66	41718.87	16.2189	0.6780	0.29525
	DSA [29]	41775.60	41699.40	NA	0.7620	0.2471
	MICA-TLA [31]	42013.08	41959.18	19.909	0.5390	NA
Case-3	CSBO	<b>41693.96</b>	41666.10	14.8500	1.7059	0.2785
	SP-DE [22]	41696.54	41668.45	15.012	1.60803	0.28092
	ECHT-DE [22]	41699.25	41671.09	15.0275	1.56188	0.28152
	SF-DE [22]	41695.55	41667.53	14.8963	1.61174	0.28022
	MSA [27]	41703.48	41675.99	15.0026	1.7236	0.27481
	MFO [27]	41707.66	41680.19	15.1026	1.7245	0.27467
	DSA [29]	41785.05	41761.22	NA	1.0573	0.2383
Case-4	CSBO	<b>0.5871</b>	48524.40	20.3134	0.58710	0.3008
	SP-DE [22]	0.59267	45549.49	18.4275	0.59267	0.30052
	ECHT-DE [22]	0.60416	46813.22	19.0821	0.60416	0.3008
	SF-DE [22]	0.59584	45246.02	18.4697	0.59584	0.30135
	DE [26]	0.5839 <sup>b</sup>	NA	NA	0.5839 <sup>b</sup>	NA
	KHA [34]	0.5810 <sup>b</sup>	42006.44	NA	0.5810 <sup>b</sup>	NA
Case-5	APFPA [30]	0.8909	43485.93	12.1513	0.8909	NA
	CSBO	<b>134934.3</b>	134934.3	57.8922	2.9658	NA
Case-6	SP-DE [22]	135055.7	135055.7	60.9596	1.0715	NA
	CSBO	<b>16.4688</b>	155741.09	16.4688	2.5323	NA
	SP-DE [22]	17.6946	155724.9	17.6946	0.8663	NA

<sup>a</sup>Load bus voltage constraint is violated, <sup>b</sup>Limits for shunt compensators are violated.

**Conflicts of interest**

The authors declare no conflicts of interest.

**References**

1. Aydin, M. (2016). Enerji verimliliğinin sürdürülebilir kalkınmadaki rolü: Türkiye değerlendirmesi. *Yönetim Bilimleri Dergisi*, 14(28), 409-441.
2. Akdag, O. (2022). A improved Archimedes optimization algorithm for multi/single-objective optimal power flow. *Electric Power Systems Research*, 206, 107796. <https://doi.org/10.1016/j.epsr.2022.107796>

3. Li, S., Gong, W., Wang, L., & Gu, Q. (2022). Multi-objective optimal power flow with stochastic wind and solar power. *Applied Soft Computing*, 114, 108045. <https://doi.org/10.1016/j.asoc.2021.108045>
4. Elattar, E. E., & ElSayed, S. K. (2019). Modified JAYA algorithm for optimal power flow incorporating renewable energy sources considering the cost, emission, power loss and voltage profile improvement. *Energy*, 178, 598-609. <https://doi.org/10.1016/j.energy.2019.04.159>
5. Akbari, E., Ghasemi, M., Gil, M., Rahimnejad, A., & Andrew Gadsden, S. (2022). Optimal power flow via teaching-learning-studying-based optimization algorithm. *Electric Power Components and Systems*,

- 49(6-7), 584-601.  
<https://doi.org/10.1080/15325008.2021.1971331>
6. Bakir, H., Guvenc, U., & Kahraman, H. T. (2022). Optimal operation and planning of hybrid AC/DC power systems using multi-objective grasshopper optimization algorithm. *Neural Computing and Applications*, 34(24), 22531-22563.  
<https://doi.org/10.1007/s00521-022-07670-y>
  7. Houssein, E. H., Hassan, M. H., Mahdy, M. A., & Kamel, S. (2023). Development and application of equilibrium optimizer for optimal power flow calculation of power system. *Applied Intelligence*, 53(6), 7232-7253.  
<https://doi.org/10.1007/s10489-022-03796-7>
  8. Ramesh, S., Verdú, E., Karunanithi, K., & Raja, S. P. (2023). An optimal power flow solution to deregulated electricity power market using meta-heuristic algorithms considering load congestion environment. *Electric Power Systems Research*, 214, 108867.  
<https://doi.org/10.1016/j.epsr.2022.108867>
  9. Premkumar, M., Kumar, C., Dharma Raj, T., Sundarsingh Jebaseelan, S. D. T., Jangir, P., & Haes Alhelou, H. (2023). A reliable optimization framework using ensembled successive history adaptive differential evolutionary algorithm for optimal power flow problems. *IET Generation, Transmission & Distribution*, 17(6), 1333-1357. <https://doi.org/10.1049/gtd2.12738>
  10. Kaur, M., & Narang, N. (2023). Optimal Power Flow Solution Using Space Transformational Invasive Weed Optimization Algorithm. *Iranian Journal of Science and Technology, Transactions of Electrical Engineering*, 1-27. <https://doi.org/10.1007/s40998-023-00592-y>
  11. Bakır, H., Guvenc, U., Duman, S., & Kahraman, H. T. (2023). Optimal power flow for hybrid AC/DC electrical networks configured with VSC-MTDC transmission lines and renewable energy sources. *IEEE Systems Journal*, 17(3), 3938 – 3949.  
<https://doi.org/10.1109/JSYST.2023.3248658>
  12. Sonmez, Y., Duman, S., Kahraman, H. T., Kati, M., Aras, S., & Guvenc, U. (2022). Fitness-distance balance based artificial ecosystem optimisation to solve transient stability constrained optimal power flow problem. *Journal of Experimental & Theoretical Artificial Intelligence*, 1-40.  
<https://doi.org/10.1080/0952813X.2022.2104388>
  13. Abd El-sattar, S., Kamel, S., Ebeed, M., & Jurado, F. (2021). An improved version of salp swarm algorithm for solving optimal power flow problem. *Soft Computing*, 25, 4027-4052.  
<https://doi.org/10.1007/s00500-020-05431-4>
  14. Jangir, P., Manoharan, P., Pandya, S., & Sowmya, R. (2023). MaOTLBO: Many-objective teaching-learning-based optimizer for control and monitoring the optimal power flow of modern power systems. *International Journal of Industrial Engineering Computations*, 14(2), 293-308.  
<https://doi.org/10.5267/j.ijiec.2023.1.003>
  15. Pandya, S. B., Ravichandran, S., Manoharan, P., Jangir, P., & Alhelou, H. H. (2022). Multi-objective optimization framework for optimal power flow problem of hybrid power systems considering security constraints. *IEEE Access*, 10, 103509-103528.  
<https://doi.org/10.1109/ACCESS.2022.3209996>
  16. Premkumar, M., Jangir, P., Sowmya, R., & Elavarasan, R. M. (2021). Many-objective gradient-based optimizer to solve optimal power flow problems: analysis and validations. *Engineering Applications of Artificial Intelligence*, 106, 104479.  
<https://doi.org/10.1016/j.engappai.2021.104479>
  17. Ghasemi, M., Akbari, M. A., Jun, C., Bateni, S. M., Zare, M., Zahedi, A., ... & Chau, K. W. (2022). Circulatory System Based Optimization (CSBO): An expert multilevel biologically inspired meta-heuristic algorithm. *Engineering Applications of Computational Fluid Mechanics*, 16(1), 1483-1525.  
<https://doi.org/10.1080/19942060.2022.2098826>
  18. Wang, L., Cao, Q., Zhang, Z., Mirjalili, S., & Zhao, W. (2022). Artificial rabbits optimization: A new bio-inspired meta-heuristic algorithm for solving engineering optimization problems. *Engineering Applications of Artificial Intelligence*, 114, 105082.  
<https://doi.org/10.1016/j.engappai.2022.105082>
  19. Abdollahzadeh, B., Gharehchopogh, F. S., & Mirjalili, S. (2021). African vultures optimization algorithm: A new nature-inspired metaheuristic algorithm for global optimization problems. *Computers & Industrial Engineering*, 158, 107408.  
<https://doi.org/10.1016/j.cie.2021.107408>
  20. Talatahari, S., & Azizi, M. (2021). Chaos game optimization: a novel metaheuristic algorithm. *Artificial Intelligence Review*, 54, 917-1004. <https://doi.org/10.1007/s10462-020-09867-w>
  21. Mohamed, A. A. A., Mohamed, Y. S., El-Gaafary, A. A., & Hemeida, A. M. (2017). Optimal power flow using moth swarm algorithm. *Electric Power Systems Research*, 142, 190-206.  
<https://doi.org/10.1016/j.epsr.2016.09.025>
  22. Biswas, P. P., Suganthan, P. N., Mallipeddi, R., & Amaratunga, G. A. (2018). Optimal power flow solutions using differential evolution algorithm integrated with effective constraint handling techniques. *Engineering Applications of Artificial Intelligence*, 68, 81-100.  
<https://doi.org/10.1016/j.engappai.2017.10.019>
  23. Zimmerman, R.D., Murillo-Sánchez, C.E., Thomas, R.J., (2023). *Matpower*.  
<http://www.pserc.cornell.edu/matpower>.
  24. MATLAB, T. U. S. G. (2022). Natick, Massachusetts: The MathWorks Inc.
  25. Zimmerman, R. D., Murillo-Sánchez, C. E., & Thomas, R. J. (2010). MATPOWER: Steady-state operations, planning, and analysis tools for power systems research and education. *IEEE Transactions on power systems*, 26(1), 12-19.  
<https://doi.org/10.1109/TPWRS.2010.2051168>
  26. Shaheen, A. M., Farrag, S. M., & El-Sehiemy, R. A. (2017). MOPF solution methodology. *IET Generation, Transmission & Distribution*, 11(2), 570-581.  
<https://doi.org/10.1049/iet-gtd.2016.1379>
  27. Mohamed, A. A. A., Mohamed, Y. S., El-Gaafary, A. A., & Hemeida, A. M. (2017). Optimal power flow using

- moth swarm algorithm. *Electric Power Systems Research*, 142, 190-206. <https://doi.org/10.1016/j.epsr.2016.09.025>
28. Boucekara, H. R., Chaib, A. E., Abido, M. A., & El-Sehiemy, R. A. (2016). Optimal power flow using an Improved Colliding Bodies Optimization algorithm. *Applied Soft Computing*, 42, 119-131. <https://doi.org/10.1016/j.asoc.2016.01.041>
29. Abaci, K., & Yamacli, V. (2016). Differential search algorithm for solving multi-objective optimal power flow problem. *International Journal of Electrical Power & Energy Systems*, 79, 1-10. <https://doi.org/10.1016/j.ijepes.2015.12.021>
30. Mahdad, B., & Srairi, K. (2016). Security constrained optimal power flow solution using new adaptive partitioning flower pollination algorithm. *Applied Soft Computing*, 46, 501-522. <https://doi.org/10.1016/j.asoc.2016.05.027>
31. Ghasemi, M., Ghavidel, S., Rahmani, S., Roosta, A., & Falah, H. (2014). A novel hybrid algorithm of imperialist competitive algorithm and teaching learning algorithm for optimal power flow problem with non-smooth cost functions. *Engineering Applications of Artificial Intelligence*, 29, 54-69. <https://doi.org/10.1016/j.engappai.2013.11.003>
32. Kumar, A. R., & Premalatha, L. (2015). Optimal power flow for a deregulated power system using adaptive real coded biogeography-based optimization. *International Journal of Electrical Power & Energy Systems*, 73, 393-399. <https://doi.org/10.1016/j.ijepes.2015.05.011>
33. Ghasemi, M., Ghavidel, S., Gitizadeh, M., & Akbari, E. (2015). An improved teaching-learning-based optimization algorithm using Lévy mutation strategy for non-smooth optimal power flow. *International Journal of Electrical Power & Energy Systems*, 65, 375-384. <https://doi.org/10.1016/j.ijepes.2014.10.027>
34. Roy, P. K., & Paul, C. (2015). Optimal power flow using krill herd algorithm. *International Transactions on Electrical Energy Systems*, 25(8), 1397-1419. <https://doi.org/10.1002/etep.1888>
35. Derrac, J., García, S., Molina, D., & Herrera, F. (2011). A practical tutorial on the use of nonparametric statistical tests as a methodology for comparing evolutionary and swarm intelligence algorithms. *Swarm and Evolutionary Computation*, 1(1), 3-18. <https://doi.org/10.1016/j.swevo.2011.02.002>



© Author(s) 2024. This work is distributed under <https://creativecommons.org/licenses/by-sa/4.0/>